Computers and Electronics in Agriculture 155 (2018) 348–358

Contents lists available at ScienceDirect

Computers and Electronics in Agriculture

journal homepage: www.elsevier.com/locate/compag

Original papers

DFT based classification of olive oil type using a sinusoidally heated, low cost electronic nose

Martin J. Oates[a], Patrick Fox[b], Lucia Sanchez-Rodriguez[c], Ángel A. Carbonell-Barrachina[c], Antonio Ruiz-Canales[a,*]

[a] Departamento de Ingeniería, Escuela Politécnica Superior de Orihuela (EPSO), Universidad Miguel Hernández de Elche (UMH), Carretera de Beniel, km 3.2, 03312 Orihuela, Alicante, Spain
[b] School of Computing, University of Leeds, Leeds LS2 9JT, United Kingdom
[c] Grupo de Investigación Calidad y Seguridad Alimentaria, Departamento Tecnología Agroalimentaria, Escuela Politécnica Superior de Orihuela (EPSO), Universidad Miguel Hernández de Elche (UMH), Carretera de Beniel, km 3.2, 03312 Orihuela, Alicante, Spain

ARTICLE INFO

Keywords:
Low cost machine olfaction
E-nose
Counterfeit food products

ABSTRACT

Low-cost electronic noses, i.e. arrays of non-specific gas sensors, have many applications for quality assessment in the food production, storage and retail industries. Classifying properties of natural products by analysing their volatile organic compound (VOC) patterns allows fraudulent and mis-represented goods to be identified and removed, before they enter the consumer market. Early results from a small study performed on olive oils demonstrate that a low cost electronic nose device based on an array of MQ-series SnO_2 gas sensors has the potential to correctly classify differing qualities of olive oils, with accuracies in the range 67–77%. Results confirm that use of sinusoidally varying heater voltage cycles on some MQ sensors improves their sensitivity, selectivity and susceptibility to drift. By using discrete Fourier transform analysis of the sensor responses, the unit discriminates between virgin/extra virgin and blended/chemically extracted pomace oils with prediction accuracies in the range 88–91%. There is also evidence that, with refinement, the unit may be capable of distinguishing among certain olive varieties. The unit can be assembled for around 30 euro.

1. Introduction

There has been much controversy in recent years over the substitution of poor quality olive oils in place of virgin and extra-virgin olive oils. In particular “pomace olive oil”, which is chemically extracted from olive pulp after normal secondary pressing (Albahari et al., 2018; IOCC, 1996), has been the subject of European Union health warnings (EU report, 2005) with respect to the potential carcinogenic properties of PAHs (polycyclic aromatic hydrocarbons) (Zha et al., 2018; Mafra et al., 2010). Therefore the development of a low cost, portable unit to assess the quality of an oil sample in the field would have commercial advantages as well as impacting positively on consumer safety (Moreira et al., 2018). Many studies of food analysis have taken place using electronic noses (for example Pascual et al., 2018; Loutfi et al., 2015; Peris and Escuder-Gilabert, 2009). Specific examples looking at characteristics such as freshness in dairy products (Abbatangelo et al., 2018; Suman et al., 2007; Schaller et al., 1999), fish (Semeano et al., 2018; Haugen et al., 2006); meat (Ramirez et al., 2018; Balasubramanian et al., 2008), fruit (Gomez et al., 2006, 2007; Zhang et al., 2008), vegetables (Cortellino et al., 2018; Riva et al., 2002), oils (Yang et al., 2018; Garcia Gonzalez and Aparicio, 2002; Gonzalez Martin et al., 2001) among others, tend to focus on the use of commercially available high-end electronic noses intended for professional laboratories only, often using offline sampling techniques. However fewer studies have been directed towards the detection of adulterated, fraudulent and misrepresented goods (Gliszczynska-Swiglo and Chmielewski, 2017) such as milk (Yu et al., 2007), peone oil (Wei et al., 2018) and olive oils (Harzalli et al., 2018; Cosio et al., 2010). Low cost prototype systems (Majchrzak et al., 2018, Changsongkram and Nimsuk, 2016; Trirongjitmoah et al., 2015; Macías Macías et al., 2013; Tang et al., 2010) employing catalytic Taguchi-type (MQ series) gas sensors, as in this study, usually focus on static heater voltages, often with highly disparate or distinctive odours.

However the datasheets for some sensors (MQ7 & MQ9 in particular) recommend switching between two (5.0 V and 1.4 V) heater voltages over a 60 + 90 s cycle, with the sensor response being sampled

* Corresponding author.
E-mail addresses: moates@btinternet.com (M.J. Oates), sc16pnf@leeds.ac.uk (P. Fox), lucia.sanchez@goumh.umh.es (L. Sanchez-Rodriguez), angel.carbonell@umh.es (Á.A. Carbonell-Barrachina), acanales@umh.es (A. Ruiz-Canales).

https://doi.org/10.1016/j.compag.2018.10.026
Received 14 July 2018; Received in revised form 13 October 2018; Accepted 16 October 2018

at the very end of the 90 s interval. This can significantly improve sensitivity as detection is now possible over a range of sensor surface temperatures. Whilst sensitivity at lower temperatures is enhanced for these sensor types, it has been shown that continuous operation at these lower temperatures allows water vapour to accumulate within the sensor material, reducing selectivity to only those gases that are water soluble (Helwig et al., 2009). More recently, there has been a move towards pulsed, sinusoidal or multi-frequency heater profiles (Vergara et al., 2009) and the use of fast Fourier transform (FFT), Discrete wavelet transform (DWT – a wavelet transform that captures both frequency and 'location in time' information), short-time Fourier transform (S-TFT – a technique that divides a long duration time signal into shorter segments of equal length and then computes the Fourier transform separately on each shorter segment. The Fourier spectra for each shorter segment can then be plotted showing the changing spectra as a function of time) and, to a lesser extent window time slicing (WTS – a technique in which the time responses of each sensor are multiplied by four smooth, bell-shaped windowing functions. The resulting traces are then integrated with respect to time and the resulting areas are used for comparison) (Yan et al., 2015). Furthermore, many previous studies have involved heating the samples to between 50 and 80 °C which can cause rapid deterioration of the sample (Daskalaki et al., 2009). All results in this report were from readings taken with the sample at room temperature (18–23 °C).

Thus, the aim of this study was to see if a low component cost electronic nose design could be sufficiently enhanced by the use of more sophisticated management and analysis software, to enable accurate classification of subtle odour differences. In particular, the classification of olive oil types. For this purpose, several metal oxide (MOQ) gas sensors were installed in a detection array of an electronic nose prototype. With this device, several samples of varied olive oils were tested. Simultaneously and in order to contrast the methodologies, a chemical analysis test was performed for the same samples. Moreover, the results and conclusions obtained from these experiments have been included in this paper.

2. Materials and methods

2.1. E-nose components

An electronic nose consists of three principal components, a sample delivery system (sampling unit), a detection array (gas detection system) and a data processing unit (pattern recognition software) (Liu et al., 2018; Gardner and Bartlett, 1999). This report focusses on preliminary results from a study using a detection array comprising 8 different MOQ gas sensors (MQ-2, MQ-3, MQ-4, MQ-5, MQ-7, MQ-8, MQ-9 and MQ-135). These are manufactured to respond to a wide range of gases, for example hydrogen, carbon monoxide, LPG, ammonia etc. (Korotcenkov, 2007; Zaretskiy et al., 2012). Whilst we are not interested in detecting these specific gases *per se*, the sensors each respond in different ways to a wide range of volatile organic compounds (VOCs) which combine to produce a unique "odour signature". As individual MQ gas sensors typically cost around 1 euro each, this allows a complete E-nose system to be built for around 30 Euros, including a simple Sample Delivery System (sample chamber with air pump or fan) and Data Processing Unit (Arduino Nano ® microcontroller with USB serial connection). Software for the Nano was developed in the Processing language using Arduino IDE® version 1.6.5. DFT analysis was performed within Microsoft Excel®. Two dimensional data visualizations (LDAnalysis plots) were produced by in-house developed software written in Visual Basic®.

Sample aliquots of 35 mL olive oil each were placed in a 135 mL glass sample chamber connected by 6 mm PVC pipe via PG7 Nylon cable glands to a separate PP5 (Food Grade Polypropylene) detection chamber containing the sensor array (see Fig. 1). Another pipe ran to a 0.4 L per min air pump, then back to the sample chamber completing a hermetically sealed loop. The sample pipe was set 8 mm above the surface of the sample, whilst the return pipe was 20 mm above the surface of the sample. Electronics hardware used in this report is based on that developed by Voodoometrics, but has been enhanced using IRF9540 Field Effect Transistors to provide hardware timer generated PWM heater control. To normalize MQ sensor outputs, 50 kohm trimpots were used as load resistors, with trim-pot values adjusted until each sensor channel gave a response of 2000 mV under steady state, "fresh air" conditions at 5 V heater voltage, at least 1 h after applying power. In addition to balancing out significantly different sensor type impedance characteristics, this also provides a degree of normalization against sensor manufacturing variabilities.

2.2. Dual heater voltage preliminary study

A preliminary study (Oates et al., 2018) which focused on the use of dual heater voltages on the MQ7, MQ9 and MQ135 sensors, also provided constant heater voltage data for the MQ2 sensor. The MQ2 showed a typical spiked response within the first 2 min of applying heater power, with the response rising to over 3000 mV before falling back to around 1900 mV. This was followed by a steady rise of between 100 and 200 mV over the next 20 min followed by a decline of 50 mV over the following 30 min under "fresh air" conditions. Long term drift effects showed more than 200 mV change over 48 h, however, changes were also seen with respect to ambient temperature and humidity variation.

In contrast, again under constant 5 V heater voltage conditions, the maximum change seen by exposing the MQ2 sensor to extra virgin oil samples was +225 mV, and for pomace olive oils, +50 mV. This response/drift characteristic provides too small a differential for absolute voltage responses to be usable for reliable oil discrimination. Further, any change in the voltage of the heater supply (caused by load current variation) was reflected in the sensor response.

2.3. Sinusoid heater based data acquisition system

By comparison, under "fresh air" conditions, typical sensor sinusoid responses under the conditions of the experiments described in this study were from 1485 mV (trough) to 2425 mV (peak), giving a 1955 mV DC offset and 940 mV peak-to-peak amplitude; for a typical pomace olive oil, 1610 mV (trough) to 2800 mV (peak), giving 2205 mV DC offset and 1190 mV peak-to-peak amplitude; and for a typical extra virgin oil, 1920 mV (trough) to 3765 mV (peak), giving 2843 mV DC offset and 1845 mV peak-to-peak amplitude. These results give much wider differential response for determining olive oil type. Whilst long term drift of DC offset was seen to exceed 400 mV, rendering absolute values of little value, many amplitude readings for oil samples were seen to show remarkable consistency. Further, some sensor responses to some oil types showed considerable deformity from a true sinusoid, suggesting a component frequency analysis technique, such as Fourier analysis, should provide further discriminatory data.

The preliminary study also determined the time constant (time for sensor reading to fall by 50% after removal of heater power under "fresh air" conditions) to be approximately 3 s, thus, a PWM period of the order of 30 ms (1% of the time constant) was used to ensure minimal temperature variation within the PWM period. Tests with an oscilloscope on the switch mode power supply (SMPS) used to provide power for the heaters showed, as expected, significant 'ringing' (decaying cycles of voltage overshoot and undershoot) after a change in load current of 1.3 A – typical of 8 sensors switching from 5 V heater voltage to 0 V. This ringing had reduced to less than 1% within 5 ms, thus, a minimum "on" time and minimum "off" time for the PWM cycle was set to be 6 ms. Failure to minimise excessive transients within the SMPS can lead to premature component failure, particularly of electrolytic capacitors (Abdi et al., 2013), and thus, the PWM was deemed to have a theoretical "safe" range of between 20% (6 ms) and 80%

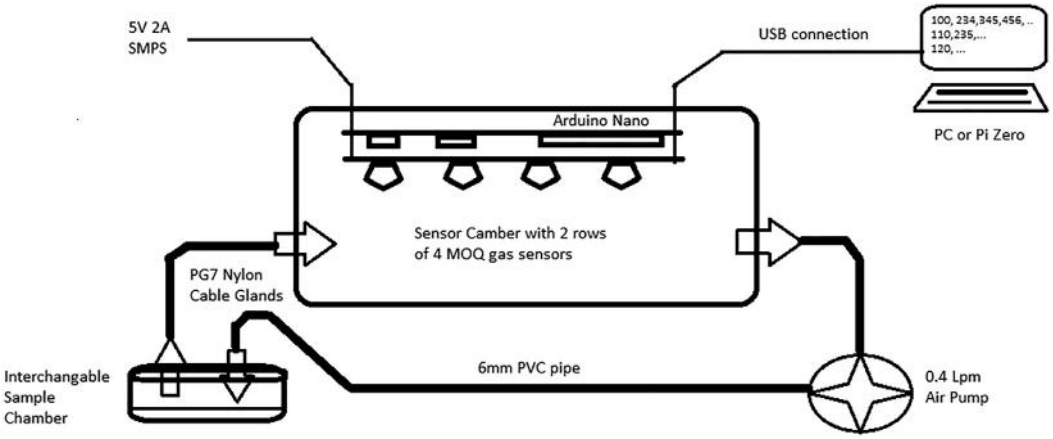

Fig. 1. Diagram of E-Nose system.

(24 ms) within a 30 ms cycle.

At a 5 V heater voltage and a typical heater resistance of 31 Ω, each sensor dissipates of the order of 800 mW raising the sensor surface to a typical value of 700 K; however for some sensor types, optimum sensitivity occurs between 550 K and 600 K (Gajdosik, 2014), and even lower for other sensor types. Based on this, and the results of the preliminary study, for the sinusoidal experiments reported on here it was decided to vary the heater power from 47% to 80% and back to 47% in 262 steps each of approximately 450 ms. Thus, the simulated sinusoidal power cycle took approximately 2 min to complete. To minimise sensor reading jitter, the 10 bit analogue to digital convertor readings were synchronised with the rising edge of the PWM heater power signal in a tight polled loop with processor interrupts disabled ensuring no more than a few microseconds of alignment variability after a fixed delay. Six readings were made in immediate succession on each of the 8 channels, the first reading after a channel change being discarded and the remaining 5 summed together producing a result in the 0–5115 range closely indicative of the sensor trim-pot voltage value in mV. Readings were temporarily stored in an array, and then output via a serial port at 57,600 baud at the end of each set of 8 sensor channel readings. These results were then stored on a PC in comma separated variable format (CSV) for later analysis. As a result of temporarily switching off processor interrupts, recorded timestamp values (nominally in tenths of a second), appear approximately 10% shorter than 'real-time' values.

Glass sample chambers containing the oils were typically connected to the system for at least 10 min, allowing 5 sinusoid cycles for data collection. Analysis was typically performed on the 4th or 5th cycle to give the oil/gas concentration time to stabilise in the sensor chamber. The whole system was flushed with fresh air for at least 10 min between samples. Multiple samples of each oil were analysed in experiments conducted over many days during a 6-month period, during which ambient temperatures varied from 18 to 23 °C, whilst humidity varied from 25% to 55%. These variations may help to explain the wide range of sensor readings seen in the "fresh air" analysis results.

2.4. Sensor coefficients and samples

Selected cycles (typically the 4th or 5th after a sample chamber containing an oil had been attached to the system) of the raw data readings for each of the 8 sensor channels were subjected to 256 element discrete Fourier transform analysis (DFT). This delivered a DC offset coefficient together with scaled pairs of real and imaginary amplitude coefficients for component cosine waves for analysed frequencies corresponding to the base frequency of the heater cycle, plus higher frequencies of integer multiples above this primary frequency. The real coefficients correspond to the amplitude of a cosine component, whilst the imaginary coefficients correspond to the amplitude of a sine component (a second sinusoid at the same frequency but at 90 degrees phase shift). An alternative representation of this complex result is to sum the squares of these components and extract the square root to deliver the amplitude of a single sinusoid, at a varying phase angle to the original heater waveform. This amplitude is herein referred to as the "Abs" value and should be divided by 128 to get the true component amplitude. The phase angle of this combined sinusoid is also determinable from the complex coefficients and is herein referred to as "Theta", given in radians. As there is discrepancy between the 262 points of the heater cycle and the 256 elements of the DFT analysis, this can be expected to produce some distortion in the frequency analysis, however effects on the first 3 frequency coefficients can be expected to be minimal.

Fourteen different, commercially sourced, Spanish olive oils were used: 4 types of extra virgin olive oil (2 of which were of named olive variety – Picual and Hojiblanca), 3 types of virgin olive oil (2 of which were of named olive variety – Picual and Hojiblanca); 3 types of blended oil; and 4 types of pomace olive oil (referred to in Spain as "*aceite de orujo*"). These are later referred to as: (for extra virgin oils) VX-O; VX-C; VX-P; VX-H; (for virgin oils) V-C; V-P; V-H; (for blended oils) B-O; B-Y; B-C; (for pomace/orujo oils) O-L; O-D; O-A; and O-C. One of the extra virgin olive oils (VX-O) was used after it had been stored in a half full bottle for over 2 years allowing self-oxidation to increase its peroxide levels (Morales et al., 1997; Bendini et al., 2009) to see if this affected E-nose readings. In all, 70 sets of eight sensor response waveforms were analysed:4 of each of VX-O, VX-P, VX-H, V-P, V-H, B-O, B-C, O-D, O-A, O-C; 5 of each of VX-C, V-C, B-Y, O-L; and 10 of fresh air.

Additionally, free fatty acid content (FFA), peroxide index (PI) and ultraviolet absorption (k232, k270 and ΔK indexes) for the 14 oil types used in this study were analysed to validate the quality of the samples. These analyses were undertaken following the specific European Union regulation (EU, 2016). Briefly, for FFA, 10 g of sample were mixed with ethanol:diethyl ether (1:1) and were neutralized with potassium hydroxide 0.1 M. Results were expressed as % of oleic acid. Peroxide index expresses quantity of peroxides in the sample that produce the oxidation of potassium iodide, so 0.5–2.0 g of sample (depending on the sample) were mixed with chloroform, acetic acid and saturated solution of IK and titrated with sodium thiosulfate 0.01 N. Results were expressed as $mEq\,O_2\,kg^{-1}$. Ultraviolet absorption measurements were undertaken with cyclohexane and quartz cuvettes using an UV–visible spectrophotometer (Helios Gamma model, UVG 1002E).

2.5. Classifiers

Decision tree classifier ruleset models were developed by using 2 dimensional visual analysis based on a relaxed greedy heuristic (Barron et al., 2008) on a randomly selected subset of half of the results, with an

Table 1
Chemical analysis results: k232, k270 and Δk; peroxide index (PI) (mEq O_2 kg^{-1}); and free fatty acid (FFA) (%) where EVOO = Extra Virgin Olive Oil and VOO = Virgin Olive Oil.

	k232	k270	Δk	Category	Pl	Category	FFA	Category
VX-O	2.33	0.17	0.02	Not EVOO	33.97	Not EVOO	0.34	EVOO
VX-C	2.30	0.14	−0.11	EVOO	12.32	EVOO	0.52	EVOO
VX-P	1.92	0.12	−0.04	EVOO	11.39	EVOO	0.28	EVOO
VX-H	1.95	0.20	−0.03	EVOO	10.05	EVOO	0.25	EVOO
V-P	2.14	0.18	−0.02	VOO	10.41	VOO	0.98	VOO
V-H	2.52	0.24	0.01	VOO	12.68	VOO	0.82	VOO
V-C	1.76	0.15	−0.01	VOO	13.49	VOO	0.42	VOO
B-O	1.75	0.29	0.04	Olive	10.53	Olive	0.39	Olive
B-Y	2.18	0.59	0.08	Olive	11.22	Olive	0.17	Olive
B-C	2.04	0.74	0.11	Olive	6.70	Olive	0.45	Olive
O-L	3.79	1.36	0.19	Not Pomace	6.83	Pomace	0.46	Pomace
O-D	4.19	1.18	0.56	Not Pomace	8.53	Pomace	0.28	Pomace
O-A	4.50	1.36	0.16	Pomace	2.38	Pomace	0.47	Pomace
O-C	3.93	1.10	0.15	Pomace	5.43	Pomace	0.56	Pomace
	k232	k270	Δk		Pl		Acidity	
	≤2.50	≤0.22	≤0.01	EVOO	≤20	EVOO	≤0.8	EVOO
	≤2.60	≤0.25	≤0.01	VOO	≤20	VOO	≤2.0	VOO
	–	≤1.15	≤0.15	Olive	≤15	Olive	≤1.0	Olive
	–	≤1.70	≤0.18	Pomace	≤15	Pomace	≤1.0	Pomace

evenly distributed selection maintained across all oil varieties. Examples of some of the generated ruleset classifiers are given in the Analysis and Discussion section. These rulesets were then used against the whole dataset to produce confusion matrices such as that presented in Table 3.

3. Results

3.1. Chemical analysis and raw sensor responses

The results of the chemical analysis tests are given in Table 1.

It is clear that the 2 years of storage induced self-oxidation has made the VX-O oil fail the delta k and peroxide index tests for an extra virgin olive oil. The blended oil B-O narrowly fails the k270 and delta k tests for a virgin olive oil whilst the other 2 blends fail by significant margins and so all 3 are correctly classified as non-virgin olive oil. The claimed pomace olive oil O-L technically fails the delta k test even for classification as a pomace oil, whilst the O-D oil fails the delta k test by a wide margin. The O-C oil technically passes the tests to allow it to be upgraded to the classification of non-virgin olive oil, rather than the lower grade of pomace.

Fig. 2 shows typical sensor response for the MQ2 and MQ3 sensors for the first hour and a half following the power up of the system. During this time the system was exposed to samples of blended oil B-O at timestamp 11,919 (1310 s), virgin Picual oil V-P at timestamp 23,083 (2539 s), pomace oil O-A at timestamp 34,356 (3779 s), and extra virgin Picual oil VX-P at timestamp 45,535 (5009 s). The MQ2 sensor response can be seen to change in both DC offset and amplitude, both typically increasing by a significant amount in the presence of higher quality oils. The MQ3 response, however is seen to decrease in amplitude and also deform in shape. The DC offset, however, increases in all cases.

3.2. Primary frequency responses

Fig. 3 shows the spread of results from the DFT analysis for the first coefficient from the MQ2 sensor across all 14 oils and “fresh air” conditions. The spreads are from different samples of each oil variety. The maximum, minimum and mean values are plotted. Both representations are shown, firstly the fixed phase Cosine and Sine amplitudes (Fig. 3a and b), and secondly the variable phase Abs amplitude and Theta phase angle (Fig. 3c and d). For higher quality oils, the first frequency MQ2 Cosine coefficients become more positive, whilst the first Sine coefficients become more negative. Alternatively, in terms of a single sinusoid, amplitudes become greater and phase shift becomes more distinct, although there is exceptionally large variation in the variable phase angle for the “fresh air” category (SD for Fresh Air being 0.143 rad vs. an average of 0.054 for the oils).

This response is similar for other sensors for example MQ7 and

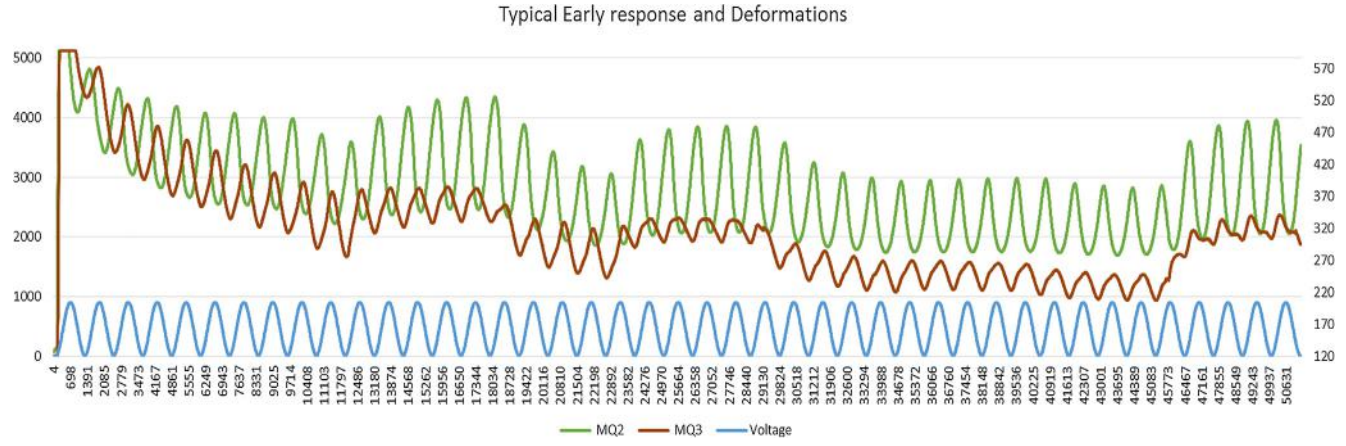

Fig. 2. Typical sinusoidal waveforms MQ2 and MQ3 deformation.

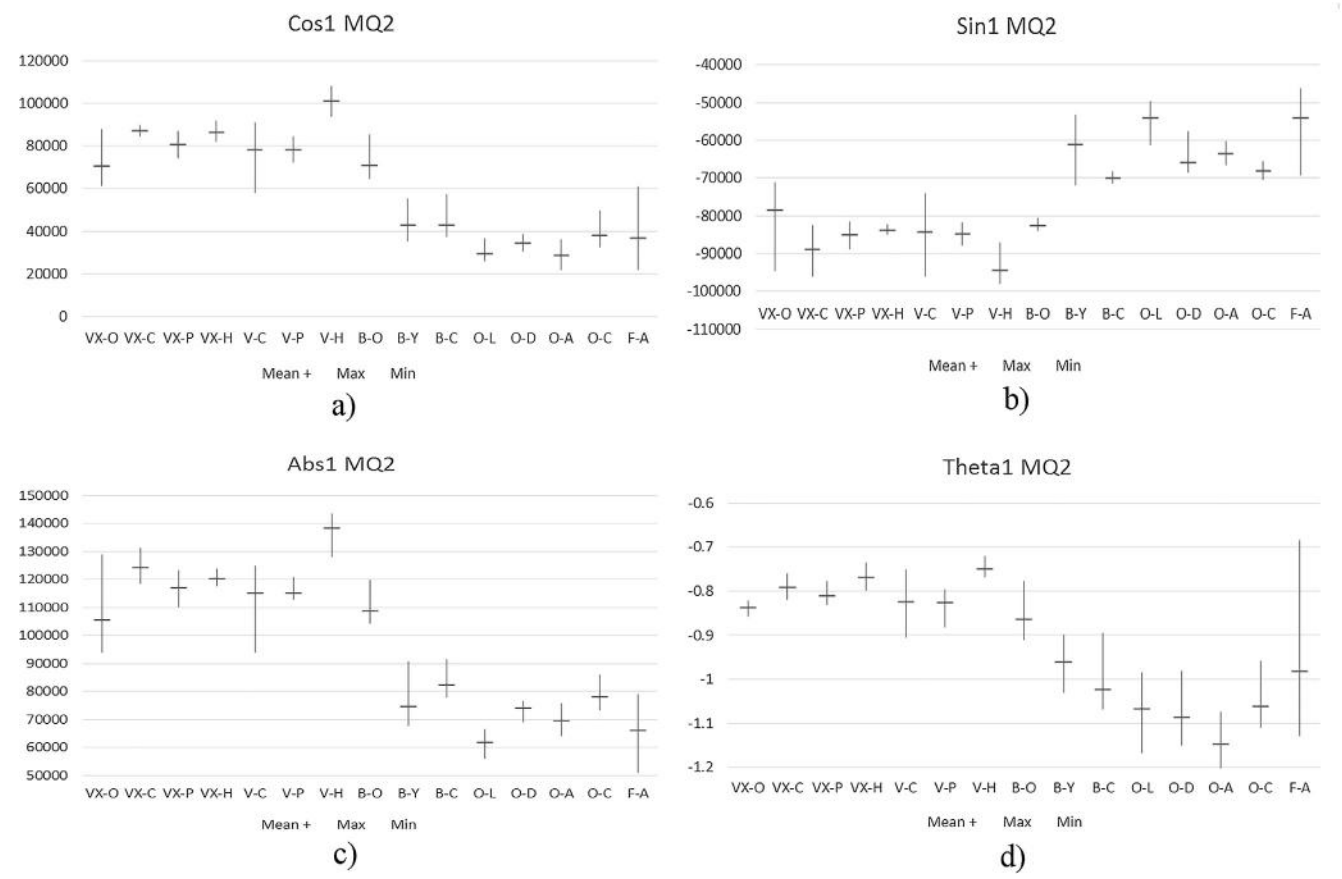

Fig. 3. a, b, c and d – MQ2 first DFT coefficient spreads (Cos, Sin, Abs and Theta).

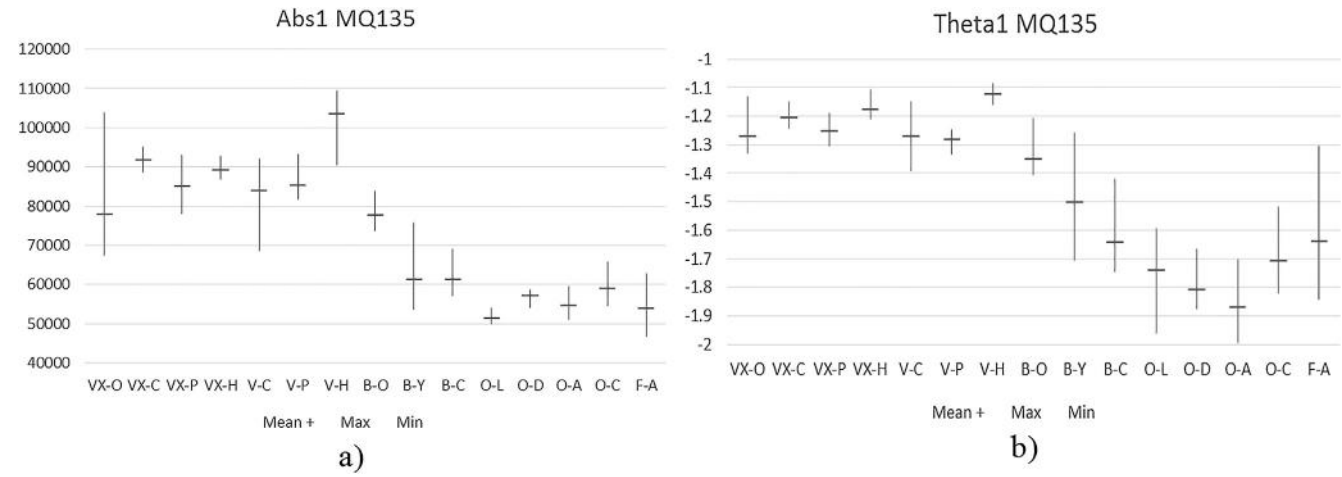

Fig. 4. a and b – MQ135 Abs1 and Theta 1.

MQ135. Fig. 4a and b show Abs1 and Theta1 for the MQ135 sensor. It is interesting to note that blended oil, B-O, shows closer similarity to virgin oils in these and the previous plots, and perhaps this is not surprising as B-O only narrowly fails the k270 and delta k tests, otherwise it could be classified as virgin from a composition view-point. This is in contrast to some results seen at the secondary frequency, see later subsection for Abs2 MQ2 and Theta2 MQ8 below. The Theta1 MQ135 (Fig. 4b) and Theta1 MQ2 (Fig. 3a) coefficients seem to favour discrimination of the Hojiblanca variety of olive (oil sample types VX-H and V-H) and this is explored in the Analysis and Discussion section.

3.3. Secondary frequency responses

Analysis of the MQ3 response waveforms shows that no clear distinction of amplitude can be observed between virgin and non-virgin oils (Fig. 5a) at the primary frequency; however, as Fig. 5b shows, deformation of the MQ3 sinusoid (represented by the amplitude of the secondary and greater frequency coefficients) is characteristic of most virgin oil samples; however extra virgin oil VX-O, virgin Picual oil V-P and blended oil B-O show significant variabilities.

For some sensors, at the secondary frequency, the amplitude of any deformation remains roughly constant across all types, but there is significant phase shift differences between oil types. This is shown here

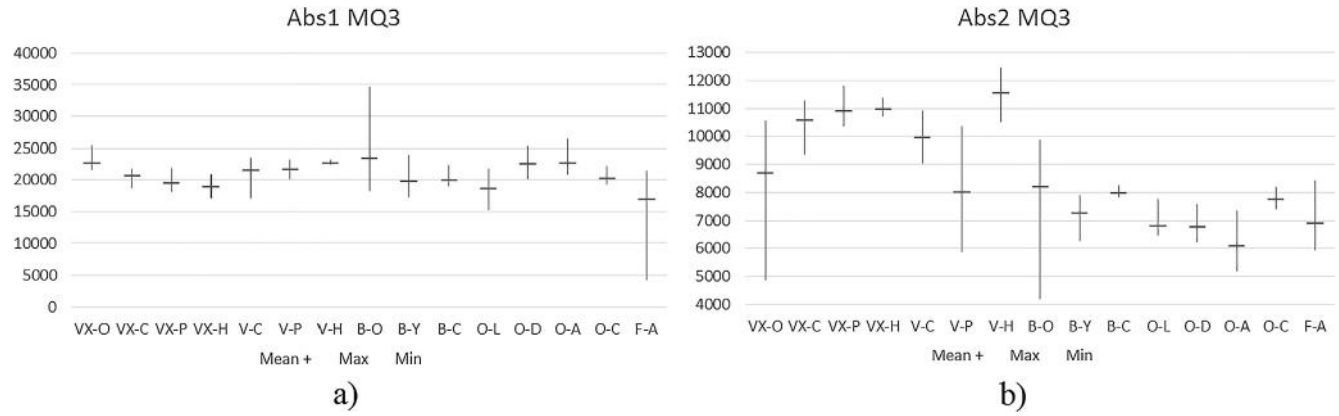

Fig. 5. a and b – Abs MQ3 spreads for first and second DFT coefficients.

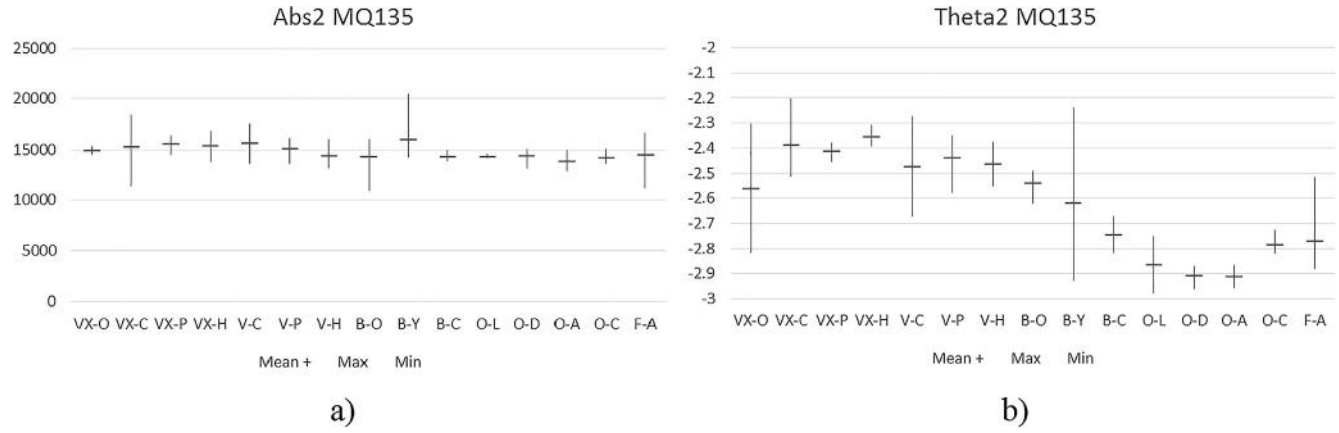

Fig. 6. a and b – MQ135 Abs2 and Theta2.

for MQ135 in Fig. 6a and b.

For other sensors (for example MQ2 and MQ8), either second frequency amplitude or secondary frequency phase shift can help distinguish between virgin and blended oils (see Fig. 7a and b).

3.4. Pomace oil detection

Although results shown so far can clearly distinguish extra virgin and virgin olive oils from pomace olive oil (orujo oil), it is important to find a coefficient (or combination of coefficients) that show that an oil specifically does contain markers from pomace oils and this is explored in the Analysis and Discussion section. This would allow detection of oils contaminated or deliberately adulterated with pomace oil that was not otherwise declared on the packaging. For this to be true, it is necessary to find a test that shows a distinct change in a sensor reading coefficient for pomace oils from the "fresh air" condition. The phase shift of the primary frequency for the MQ4 sensor appears to show this, whereby the variable phase angle "Theta1", is seen to generally become more negative for pomace oils than under "fresh air" conditions, see Fig. 8a. This is also true to a less defined extent with Theta1 MQ8 (see Fig. 8b). Higher quality oils give less negative phase readings, whilst blended oils give results which straddle both positions.

Further work is needed to see if the large variability in test results for the same oil type can be reduced, and this is discussed in the following section; however, variability across sensor types and coefficients is not uniform as is demonstrated by Fig. 3d for the MQ2 sensor (or 4b

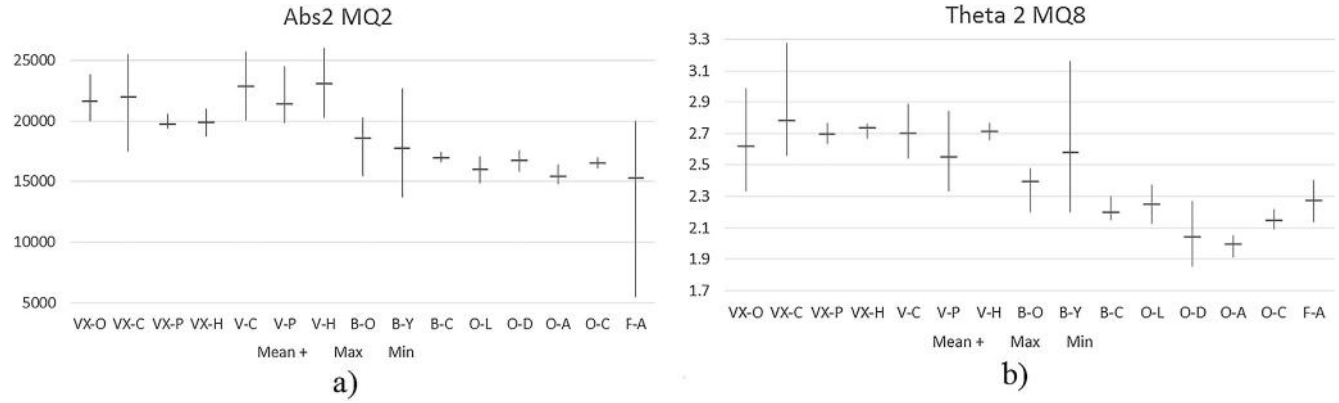

Fig. 7. a and b – Abs2 MQ2 and Theta2 MQ8.

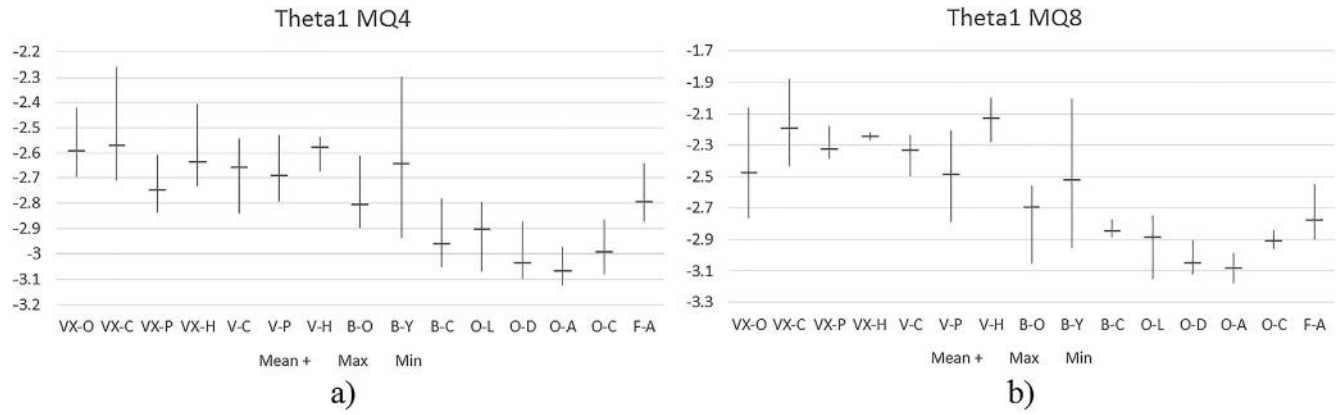

Fig. 8. a and b – Specific detection of pomace oils by MQ4 and MQ8 Theta1 coefficients.

for MQ135) where, in contrast to Fig. 7a (or 6b for MQ135), low variability is seen in higher quality oil samples with larger variability seen in poorer quality oils.

4. Analysis and discussion

This section discusses ways in which the sensor DFT coefficient results can be used to determine olive oil type and variety by using decision tree ruleset classifiers. It also examines in more detail the high levels of variation seen in some of the sensor coefficients for "fresh air", discussing possible causes for this and suggesting possible solutions to be explored in future experiments.

4.1. ANOVA results for oil type determination

Fig. 3 shows that it is possible to determine whether an oil sample is virgin (including extra virgin and virgin oils) or pomace oils based only on the MQ2 first frequency responses, there being no overlap between Abs1 MQ2 readings in the virgin and pomace categories. This is corroborated by other sensor responses (for example Fig. 4 for MQ135). When the Abs1 MQ2 coefficient values were grouped into 5 classes: extra virgin; virgin; blends; pomace and fresh air, this gave typical group sizes of 14 samples, for which the mean and sample standard deviation were calculated. These results are given in Table 2. For a normal distribution, 98% of the population can be expected to lie within plus or minus 2.33 standar deviations of the mean. Table 2 shows that the lowest value of mean −2.33 standard deviations for extra virgin and virgin oils is 89823.67, implying that less than 1% of the true population would give readings lower than this value, whilst the highest value of mean +2.33 standard deviations for pomace oil was 89565.17 implying that less than 1% of the true population would give readings greater than this value. As these two limits do not overlap, this gives a good degree of confidence that the value of this coefficient can be used to distinguish between virgin/extra virgin and pomace olive oils. Blended oils, however, had a much wider variance, and as the non-overlap limit between lowest mean −1 standard deviation for extra virgin is at 105,787, this leaves a projected 16% of the true population below this value, and for highest mean +1 standard deviation for blended Oils at 105767.7 this leaves 16% above this value, assuming normal distributions.

Considering the Abs1 MQ2 sensor coefficients for the 5 classes (extra virgin, virgin, blends, pomace and fresh air), there was a statifically significant difference between the groups as determined by one-way ANOVA which delivered a p value of less than 0.001. According to Tukey's least significant difference test, values for clasess extra virgin and virgin, and classes pomace and fresh air, were not significantly different ($p > 0.05$) in themselves, supporting the hypothesis that the data can be considered to come from 3 significantly different classes: "extra virgin & virgin", "blends" and "pomace and fresh air".

Specific detection and classification of blended oils as a class based on sensors readings is clearly more problematic – all three brands sampled here are classified as non-virgin by chemical analysis. However, the use of second frequency coefficients such as Abs2 MQ2 and Theta2 MQ8 (Fig. 7a and b) show some possibilities for discrimination, particularly for oil B-O. It is perhaps not surprising that different brands of blended oils show such differences, as the fact that they do not have to conform to the European standards for virgin and extra virgin oils, allows significant flexibility in their composition.

4.2. Ruleset classifiers

Based on visual inspection of individual coefficients, it is not possible to separate extra virgin samples from virgin. However, there are clearly subtle differences between the response of each sensor; for example, Abs1 MQ3 and Theta1 MQ2, and more detailed analysis of the results exposes weighted combinations of coefficients which allows

Table 2
Statistical analysis of MQ2 Abs1 results.

MQ2 Abs1		Virgin Extra	Virgin	Blends	Orujos	Fresh Air
	Mean	116883.9	123013.5	88736.1	71057.5	66182.83
	Stnd Dev	11096.96	14244.58	17031.56	7943.204	11445.79
68%	Mean + 1 SD	127980.9	137258.1	105767.7	79000.71	77628.63
	Mean − 1 SD	105,787	108,769	71704.53	63114.3	54737.04
95%	Mean + 2 SD	139077.9	151502.7	122799.2	86943.91	89074.42
	Mean − 2 SD	94690.02	94524.38	54672.97	55171.1	43291.24
98%	Mean + 2.33	142739.9	156203.4	128419.6	89565.17	92851.53
	Mean − 2.33	91028.03	89823.67	49052.55	52549.84	39514.13
99%	Mean + 2.576	145469.7	159707.6	132609.4	91519.2	95667.2
	Mean − 2.576	88298.17	86319.51	44862.79	50595.81	36698.47
99.70%	Mean + 3 SD	150174.8	165747.3	139830.8	94887.12	100520.2
	Mean − 3 SD	83593.06	80279.81	37641.4	47227.89	31845.45

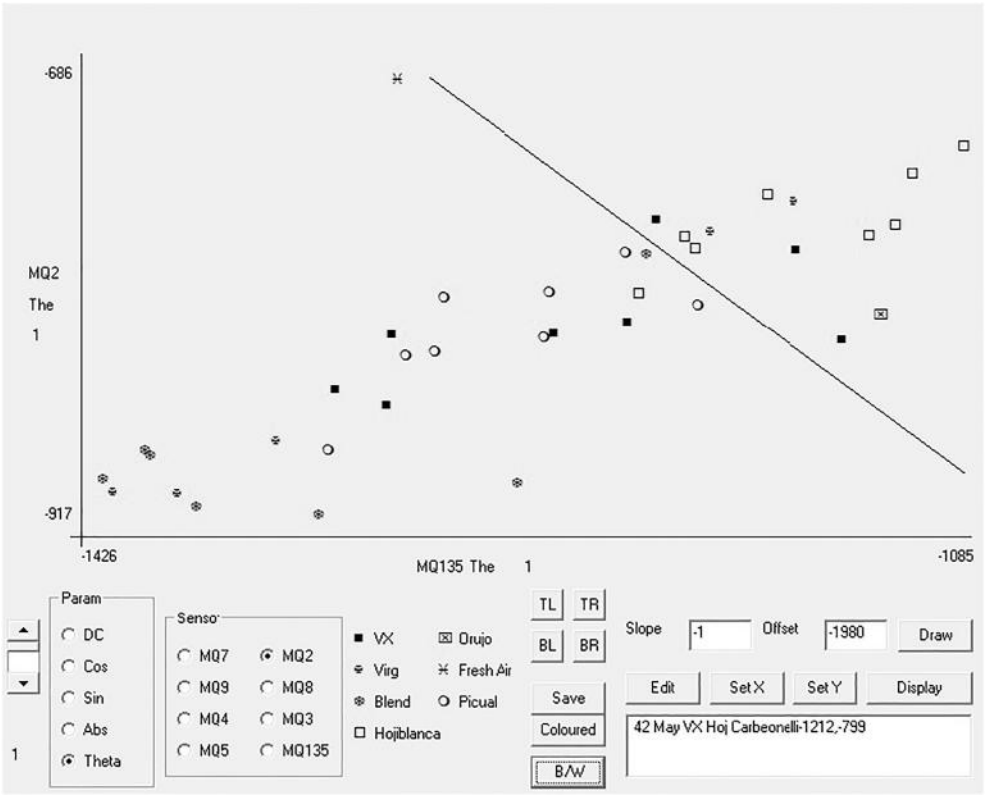

Fig. 9. Separation of olive varieties using MQ135 Theta1 and MQ2 Theta1.

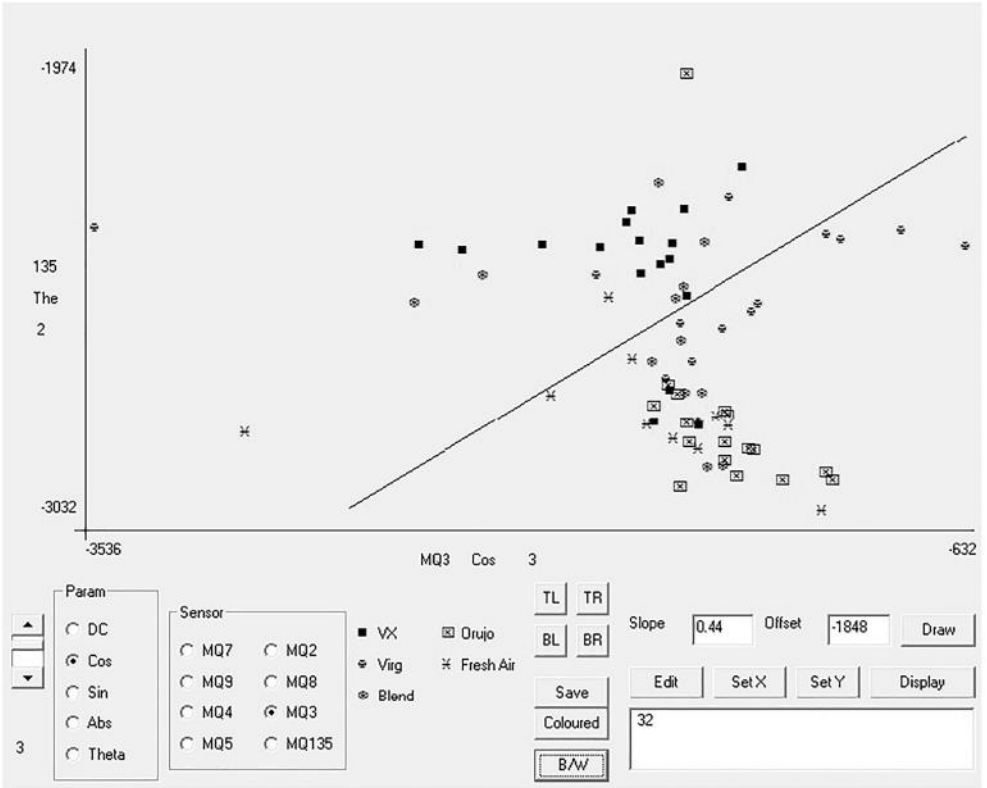

Fig. 10. Separation of oil types using MQ3 Cos3 and MQ135 Theta2.

Table 3
Confusion matrix classification results.

Classifier O/P	Fresh Air	Pomace	Blend	Virgin	Extra		
Actual							
Fresh Air	8	1	1			8/10	80%
Pomace	3	13	1			13/17	76%
Blend	1	3	6	1	2	6/13	46%
Virgin				10	3	10/13	77%
Extra			1	2	14	14/17	82%
Correct	8/12	13/17	6/9	10/13	14/19	51/70	73%
Accuracy	67%	76%	67%	77%	74%	73%	Overall
V&X vs B&P	4	< Wrong >	3	< Wrong >	3		
	8/12	< Correct >	23/26	< Correct >	29/32	60/70	
	67%	< Accuracy >	88%	< Accuracy >	91%	86%	Overall

greater distinction to be made. Indeed, results from Figs. 3d, and 4b suggest that it is possible to distinguish oils made of the Hojiblanca variety of olive from the Picual variety, which is shown in Fig. 9. Of the 16 samples specifically of these 2 varieties, the unit correctly classified the 8 samples of Picual, and 7 of the 8 samples of Hojiblanca, delivering a prediction accuracy of 93.75% using a simple classifier based on MQ2 Theta1 + MQ135 Theta1, the resulting value being greater than or less than −1.98. Against the null hypothesis of a 50:50 prediction, from the 65,536 possible outcomes, only 17 could be considered better or the same, delivering a 1 in 3855 likelihood based on random chance. With a probability value lower than 0.00026, it is reasonable to reject the null hypothesis (see Fig. 10).

As another example, the confusion matrix results in Table 3 can be achieved using the simple decision tree classifier based on only 6 coefficients (MQ2 Abs1, MQ5 Cos1, MQ3 Cos3, MQ135 Theta2, MQ4 Abs3 and MQ9 Theta2):

```
If MQ2 Abs1 > 89800 Then
  If MQ5 Cos1 < -51500 Then
    CLASS = BLEND
  ElseIf MQ5 Cos1 > -25000 Then
    CLASS = POMACE
  Else
    If (MQ3 Cos3 - 4200) > (2260 * MQ135 Theta2) Then
   CLASS = VIRGIN Else CLASS = EXTRA
  End If
Else
  If MQ4 Abs3 < 630 Then
    If MQ9 Theta2 < -2.6 Then CLASS = POMACE Else
   CLASS = BLEND
  Else
    If MQ4 Abs3 > 540 Then CLASS = FRESH AIR Else
   CLASS = BLEND
  End If
End If
```

This delivers a correct classification of extra virgin 74% of the time, of virgin 77% of the time, of blend 67% of the time, of pomace 76% of the time, and of fresh air 67%, giving an overall classification accuracy of 73%. If, "virgin and extra virgin" and "pomace and blend" samples are grouped in two categories, then, the classification of "virgin/extra virgin" is correct 91% of the time, and of "pomace/blend" is also correct 88% of the time, an overall accuracy of 86%. Additionally, the classifier can be simplified to using only 3 coefficients (MQ2 Abs1, MQ5 Cos1 and MQ4 Abs3) to:

```
If MQ2 Abs1 > 89800 Then
  If MQ5 Cos1 < -51500 or > -25000 Then
    CLASS = BLEND/POMACE Else CLASS = VIRGIN/EXTRA
Else
  If MQ4 Abs3 > 540 Then CLASS = FRESH AIR Else
    CLASS = BLEND/POMACE
End If
```

An example of separation of oil types using MQ3 Cos3 (plotted on the X axis) and MQ135 Theta2 (plotted at *1000 on the Y axis) can be seen in Fig. 10. Values of x = MQ3 Cos3, y = MQ135 Theta2 (*1000) which lie above or to the left of a diagonal line defined by y = (x − 4200)/2.26 are predominantly from extra virgin olive oils, whilst those lying below or to the right of this line are from virgin oils (the classifier would have already eliminated most other oil types with the preceding MQ2 Abs1 and MQ5 Cos1 tests).

4.3. Fresh air variability

The large variability of "fresh air" readings may be due to variability of air temperature and humidity, precise details of which were not recorded at the time of the experiments. Preliminary analysis of results for typical high variability sensor coefficients (for example Abs1 MQ3, Abs2 MQ2, Theta1 MQ2 and Theta1 MQ135) against estimated air temperature and humidity do not show strong correlation, with the magnitudes of correlation coefficient all below 0.52 with some below 0.2. However other sensor coefficients do show significant correlation, for example with temperature: Theta2 MQ8 at −0.717; and with humidity: Sin2 MQ135 at 0.816; Theta2 MQ8 at −0.720 and Theta2 MQ2 at −0.869 being the most significant. These particular sensor coefficients do not however demonstrate particularly wide variability for "fresh air" samples. Some sensor types are known to be susceptible to the airborne odours of citrus fruits, perfumes and domestic cleaning agents etc. any of which could have been present in the air in different concentrations on different days during experimental runs. In future experiments, an activated carbon filter will be used on the fresh air supply to reduce the possibility of these effects.

Many results for VX-O (the oldest oil sample) show significant variability. Preliminary analysis, including estimated age and temperature of sample, show no obvious correlation. One possibility is due to potential variation in ambient UV radiation, possibly from sunlight or fluorescent illumination, as this has been shown to significantly affect the sensitivity of some sensors (Saboor et al., 2016).

This variability is also true for some coefficients of B-O, which tends to give results more typical of virgin oils than pomace oils. However, chemical analysis of B-O does show that it is indeed close to formal classification as a virgin oil. Further, blended oil B-Y shows significant variability for several coefficients.

4.4. Future improvements and applications

For future experiments: the number of points in the heater cycle should be fully aligned with the DFT analysis; a wider range of PWM swing should be tried (20%–80%–20%) (however extending this invokes a trade-off between enhanced temperature operating range and

response time at any particular temperature, or extending the overall cycle time); and improvements made to reduce potential effects from environmental factors such as UV light levels and "fresh air" contaminants such as operating the equipment in a UV opaque enclosure and using activated carbon filters on the fresh air supply. Specific measurements of air temperature and humidity and sample temperature must be made, possibly using a DHT22 sensor in the sensor chamber and a waterproof DS18B20 sensor in the sample chamber. Whilst DFT analysis requires more computing power than is practically available on the Arduino Nano®, the PC can easily be replaced by a low cost 32 or 64 bit processor system such as a Raspberry Pi Zero® with local SD card storage and a small LCD display, raising total component costs from 30 euro to around 50 euro. If only MQ3 sensors continue to show significant sinusoidal deformity, it may be possible to use simpler analysis methods, such as noting peaks and troughs of responses to assess amplitude and phase. This would then be possible within the Arduino 8® bit-processor alone.

The next stage of the project is to build four more units to test the manufacturing repeatability of the MQ sensors. Once complete, field trials are planned for a range of applications using this technology including detection of effluent treatment plant malfunction and beehive monitoring, to see if there is any correlation between hive and/or locality VOC profiles and the early onset of Nosema Ceranae, believed to be linked to beehive de-population. The data could also assist in hive logistics with respect to optimal placement and timing for both crop pollination and honey production. The extensive (currently around 1.5 million data points) raw sensor value datasets will be made publicly available after publication to facilitate additional analysis.

5. Conclusions

Based on these results, the unit appears capable of a high degree of accurate prediction (in the region of 90%) when asked to distinguish between the group "virgin/extra virgin" and the group "blend/pomace" oils. If more detailed prediction is required, accuracies decline to the 67–77% range. However a specific test to discriminate between the Hojiblanca and Picual olive varieties, based on the phase variation of MQ2 and MQ135 responses, delivered a 93.75% success rate with a probability against random chance of less than 0.00026. This is a significant beyond the 3 sigma level.

The use of sinusoidal heater voltages clearly improves the sensitivity of some commercially available MOQ sensors and their response/drift ratios. Improved selectivity is clearly seen in MQ3 response waveforms, whilst DFT analysis shows there is information content relevant to olive oil classification in many higher order frequency coefficients.

Despite the low component costs and general simplicity of this device, the use of more sophisticated software techniques such as sinusoidal sensor excitation schedules and DFT data analysis methods, seem to achieve some noteworthy results. Whilst not delivering any form of recognised chemical composition analysis, by effective pattern matching, the device can be trained to recognize a range of "odour signatures". Given its low cost, the device clearly has significant potential in many other fields of study.

Further experiments are planned in which air temperature and humidity, and oil sample temperature will be recorded to see if compensation is possible to reduce sample response variability.

Acknowledgements

The second author would like to thank the research charity EvoSolve (Uk Reg 1086384/4107114) for financial assistance during the execution of this work.

References

Abbatangelo, M., Nunez-Carmona, E., Sberveglieri, V., Zappa, D., Comini, E., Sberveglieri, G., 2018. Application of a novel S3 nanowire gas sensor device in parallel with GC-MS for the identification of rind percentage of grated parmigiano Reggiano. Sensors 18 (5). https://doi.org/10.3390/s18051617.

Abdi, B., Ghasemi, R., Mirtalaei, S.M.M., 2013. The effect of electrolytic capacitors on SMPS's failure rate. Int. J. Mach. Learn. Comput. 3 (3), 300–304.

Albahari, P., Jug, M., Radic, K., Jurmanovic, S., Brncic, M., Brncic, S.R., Cepo, D.V., 2018. Characterization of olive pomace extract obtained by cyclodextrin-enhanced pulsed ultrasound assisted extraction. LWT-Food Sci. Technol. 92, 22–31. https://doi.org/10.1016/j.lwt.2018.02.011.

Balasubramanian, S., Panigrahi, S., Logue, C.M., Doetkott, C., Marchello, M., Sherwood, J.S., 2008. Independent component analysis-processed electronic nose data for predicting *Salmonella Typhimurium* populations in contaminated beef. Food Control 19, 236–246.

Barron, A.R., Albert Cohen, A., Dahmen, W., DeVore, R.A., 2008. Approximation and learning by greedy algorithms. Ann. Stat. 36 (1), 64–94.

Bendini, A., Cerretani, L., Salvador, M., Fregapane, G., Lercker, G., 2009. Stability of the sensory quality of virgin olive oil during storage: an overview. Ital. J. Food Sci. 21, 389–406.

Chansongkram, W., Nimsuk, N., 2016. Development of a wireless electronic nose capable of measuring odors both in open and closed systems. Proc. Comput. Sci. 86, 192–195.

Cortellino, G., Gobbi, S., Rizzolo, A., 2018. Shelf life of fresh-cut lamb's lettuce (*Valerianella locusta* L.) monitored by electronic nose and relationship with chlorophyll a fluorescence and mechanical-acoustic test. Postharvest Biol. Technol. 136, 178–186. https://doi.org/10.1016/j.postharvbio.2017.11.002.

Cosio, M.S., Benedetti, S., Buratti, S., Scampicchio, M., Mannino, S., 2010. Application of the electronic nose in olive oil analyses. In: Olives and Olive Oil in Health and Disease Prevention, pp. 553–559 (Chapter 60).

Daskalaki, D., Kefi, G., Kotsiou, K., Tasioula-Margari, M., 2009. Evaluation of phenolic compounds degradation in virgin olive oil during storage and heating. J. Food Nutr. Res. 48 (1), 31–41.

European Commission report 2005. <http://mie.esab.upc.es/ms/formacio/ControlContaminacioAgricultura/biblio/> contaminaci olis vegetals per PAH UE. pdf.

EU regulations, 2016. REGLAMENTO DELEGADO (UE) 2016/2095 DE LA COMISIÓN de 26 de septiembre de 2016 que modifica el Reglamento (CEE) n.o 2568/91, relativo a las características de los aceites de oliva y de los aceites de orujo de oliva y sobre sus métodos de análisis, 1.12.2016 L 326/1.

Gajdosik, L., 2014. The derivation of the electrical conductance/temperature dependency for tin dioxide gas sensor. Adv. Electr. Electron. Eng. 12 (5), 529–536.

Garcia Gonzalez, D.L., Aparicio, R., 2002. Detection of vinegary defect in virgin olive oils by metal oxide sensors. J. Agric. Food Chem. 50, 1809–1814.

Gardner, J., Bartlett, P., 1999. Electronic Noses, Principles and Applications. Oxford University Press, New York, NY, USA.

Gliszczynska-Swiglo, A., Chmielewski, J., 2017. Electronic nose as a tool for monitoring the authenticity of food. A review. Food Anal. Methods 10 (6), 1800–1816. https://doi.org/10.1007/s12161-016-0739-4.

Gomez, A.H., Hu, G.X., Wang, J., Pereira, A.G., 2006. Evaluation of tomato maturity by electronic nose. Comput. Electron. Agri. 54, 44–52.

Gomez, A.H., Wang, J., Hu, G.X., Pereira, A.G., 2007. Discrimination of storage shelf-life for mandarin by electronic nose technique. LWT-Food Sci. Technol. 40, 681–689.

Gonzalez Martin, Y., Cerrato Oliveros, M.C., Perez Pavon, J.L., Garcia Pinto, C., Moreno Cordero, B., 2001. Electronic nose based on metal oxide semiconductor sensors and pattern recognition techniques: characterisation of vegetable oils. Anal. Chim. Acta 449, 69–80.

Harzalli, U., Rodrigues, N., Veloso, A.C.A., Dias, Luis G., Pereira, J.A., Oueslati, S., Peres, A.M., 2018. A taste sensor device for unmasking admixing of rancid or winey-vinegary olive oil to extra virgin olive oil. Comput. Electron. Agric. 144, 222–231. https://doi.org/10.1016/j.compag.2017.12.016.

Haugen, J.E., Chanie, E., Westad, F., Jonsdottir, R., Bazzo, S., Labreche, S., Marcq, P., Lundby, F., Olafsdottir, G., 2006. Rapid control of smoked Atlantic salmon (*Salmo salar*) quality by electronic nose: correlation with classical evaluation methods. Sens. Actuat. B 116, 72–77.

Helwig, A., Muller, A.G., Sberveglieri, G., Eickhoff, M., 2009. On the low-temperature response of semiconductor gas sensors. J. Sens. (Hindawi) 17pp. Article ID 620720.

IOOC (International Olive Oil Council), 1996. COI/T.20/Document 15/Rev. 1 Organoleptic Assessment of Olive Oil. Resolution RES-3/75-IV/96. 20 November.

Korotcenkov, G., 2007. Metal oxides for solid-state gas sensors: what determines our choice? Mater. Sci. Eng., B 139, 1–23.

Liu, Q., Zhao, N., Zhou, D.D., Sun, Y., Sun, K., Pan, L.Q., Tu, K., 2018. Discrimination and growth tracking of fungi contamination in peaches using electronic nose. Food Chem. 262, 226–234. https://doi.org/10.1016/j.foodchem.2018.04.100.

Loutfi, A., Coradeschi, S., KumarMani, G., Shankar, P., Balaguru Rayappan, J.B., 2015. Electronic noses for food quality: a review. J. Food Eng. 144, 103–111.

Macías Macías, M., Agudo, J.E., García Manso, A., García Orellana, C.J., González Velasco, H.M., Gallardo Caballero, R.A., 2013. Compact and low cost electronic nose for aroma detection. Sensors 13, 5528–5541.

Mafra, I., Amaral, J.S., Oliveira, M.B.P.P., 2010. Polycyclic aromatic hydrocarbons (PAH) in olive oils and other vegetable oils; potential for carcinogenesis. In: Olives and Olive Oil in Health and Disease Prevention, pp. 489–498 (Chapter 54).

Majchrzak, T., Wojnowski, W., Dymerski, T., Gebicki, J., Namiesnik, J., 2018. Electronic noses in classification and quality control of edible oils: a review. Food Chem. 246, 192–201. https://doi.org/10.1016/j.foodchem.2017.11.013.

Morales, M.T., Rios, J.J., Aparicio, R., 1997. Changes in the volatile composition of virgin olive oil during oxidation: flavour and off-flavours. J. Agric. Food Chem. 45, 2666–2671.

Moreira, A.C.D., Machado, A.H.D., de Almeida, F.V., Braga, J.W.B., 2018. Rapid purity

determination of copaiba oils by a portable NIR spectrometer and PLSR. Food Anal. Methods 11 (7), 1867–1877. https://doi.org/10.1007/s12161-017-1079-8. SI.
Oates, M., Madsen, M., Cuenca, Roca O., Fernández, López A., Ruiz-Canales, A., 2018. Preliminary results from olive oil classification system using a low cost electronic nose. Proceedings of SNIH18, Feb 2018. Lugo (Spain).
Pascual, L., Gras, M., Vidal-Brotons, D., Alcaniz, M., Martinez-Manez, R., Ros-Lis, J.V., 2018. A voltammetric e-tongue tool for the emulation of the sensorial analysis and the discrimination of vegetal milks. Sens. Actuat. B-Chem. 270, 231–238. https://doi.org/10.1016/j.snb.2018.04.151.
Peris, M., Escuder-Gilabert, L., 2009. A 21st century technique for food control: electronic noses. Anal. Chim. Acta 638 (1), 1–15 Elsevier.
Ramirez, H.L., Soriano, A., Gomez, S., Iranzo, J.U., Briones, A.I., 2018. Evaluation of the Food Sniffer electronic nose for assessing the shelf life of fresh pork meat compared to physicochemical measurements of meat quality. Eur. Food Res. Technol. 244 (6), 1047–1055. https://doi.org/10.1007/s00217-017-3021-0.
Riva, M., Benedetti, S., Mannino, S., 2002. Shelf life of fresh cut vegetables as measured by an electronic nose: preliminary study. Ital. Food Tech. 27, 5–11.
Saboor, F.H., Ueda, T., Kamada, K., Hyodo, T., Mortazavi, Y., Khodadadi, A.A., Shimizu, Y., 2016. Enhanced NO_2 gas sensing performance of bare and Pd-loaded SnO_2 thick film sensors under UV-light irradiation at room temperature. Sens. Actuat. B: Chem. 223, 429–439.
Schaller, E., Bosset, J.O., Escher, F., 1999. Practical experience with 'Electronic Nose' systems for monitoring the quality of dairy products. Chimia 53, 98–102.
Semeano, A.T.S., Maffei, D.F., Palma, S., Li, R.W.C., Franco, B.D.G.M., Roque, A.C.A., Gruber, J., 2018. Tilapia fish microbial spoilage monitored by a single optical gas sensor. Food Control 89, 72–76. https://doi.org/10.1016/j.foodcont.2018.01.025.
Suman, M., Riani, G., Dalcanale, E., 2007. MOS-based artificial olfactory system for the assessment of egg products freshness. Sens. Actuat. B 125, 40–47.
Tang, K., Chiu, S., Pan, C., Hsieh, H., Liang, Y., Liu, S., 2010. Development of a portable electronic nose system for the detection and classification of fruity odors. Sensors 10, 9179–9193.
Trirongjitmoah, S., Juengmunkong, Z., Srikulnath, K., Somboon, P., 2015. Classification of garlic cultivars using an electronic nose. Comput. Electron. Agric. 113, 148–153.
Vergara, A., Vilanova, X., Llobet, E., 2009. Dynamic methods for improving the performance of semiconductor gas sensors. In: Intelligent Systems: Techniques and Applications (Shaker), pp. 133–169 (Chapter 5).
Wei, X., Shao, X., Wei, Y., Cheong, L., Pan, L., Tu, K., 2018. Rapid detection of adulterated peony seed oil by electronic nose. J. Food Sci. Technol. 55 (6), 2152–2159. https://doi.org/10.1007/s13197-018-3132-z. (in press).
Yan, J., Guo, X., Duan, S., Jia, P., Wang, L., Peng, C., Zhang, S., 2015. Electronic nose feature extraction methods: a review. Sensors 15, 27804–27831.
Yang, Y., Zhao, C., Tian, G., Lu, C., Li, C., Bao, Y., Tang, Z., McClements, D.J., Xiao, H., Zheng, J., 2018. Characterization of physical properties and electronic sensory analyses of citrus oil-based nanoemulsions. Food Res. Int. 109, 149–158. https://doi.org/10.1016/j.foodres.2018.04.025.
Yu, H.C., Wang, J., Xu, Y., 2007. Identification of adulterated milk using electronic nose. Sens. Mater. 19, 275–285.
Zaretskiy, N.P., Menshikov, L.I., Vasiliev, A.A., 2012. Theory of gas sensitivity of nanostructured MOX layers: charge carrier self-exhaustion approach. Sens. Actuat. B 175, 234–245.
Zha, Y., Zhang, Y.L., Ma, Z.L., Tang, J., Sun, K., 2018. Distribution, seasonal variations and ecological risk assessment of polycyclic aromatic hydrocarbons in foliar dust of Nanjing, China. Bull. Environ. Contam. Toxicol. 100 (4), 560–569. https://doi.org/10.1007/s00128-018-2287-7.
Zhang, H., Chang, M., Wang, J., Ye, S., 2008. Evaluation of peach quality indices using an electronic nose by MLR, QPST and BP network. Sens. Actuat. B Chem. 134, 332–338.